Dimensioning and Configuration of EES Systems for Electric Vehicles with Boundary-Conditioned Adaptive Scalarization

Wanli Chang, Martin Lukasiewycz, Sebastian Steinhorst
TUM CREATE, Singapore
wanli.chang@tum-create.edu.sg

Samarjit Chakraborty
TU Munich, Germany
samarjit@tum.de

ABSTRACT

Electric vehicles (EVs) are widely considered as a solution for efficient, sustainable and intelligent transportation. An electrical energy storage (EES) system is the most important component in an EV in terms of performances and cost. This work proposes an approach for optimal dimensioning and configuration of EES systems in EVs. It is challenging to find optimal design points in the parameter space, which expands exponentially with the number of battery types available and the number of cells that can be implemented for each type. A multi-objective optimization problem is formulated with the driving range, rated power output, installation space and cost as design targets. We report a novel boundary-conditioned adaptive scalarization technique to solve both convex and concave problems. It provides a Pareto surface of evenly distributed Pareto points, presents the group of Pareto points according to different specific requirements from automotive manufacturers and also takes the fact in EES system design into account that the importance of an objective could be nonlinear to its value. Numerical and practical experiments prove that our proposed approach is effective for industry use and produces optimal solutions.

1. INTRODUCTION

Electric vehicles (EVs) are prevailingly considered as an efficient and sustainable solution for transportation in the future [1]. However, currently the weak point of EVs remains the electrical energy storage (EES), i.e., the battery [2]. Very often, the purchase decision of customers depends on the driving range that is strongly correlated to the capacity and mass of the EES system. It is also desirable to have excellent acceleration capabilities within a wide range of velocity, which is determined by the power output of the EES system. At the same time, the EES system is the most expensive component in EVs due to high costs of materials and production processes. Therefore, the optimal design of EES systems for EVs in terms of dimensioning and configuration becomes a challenging task within the entire automotive design chain.

In recent years, battery technology has progressed from Lead-acid via Nickel-Metal Hydride (NiMH) to Lithium-Ion (Li-Ion). Currently, the Li-Ion technology is dominating the market in those segments where high energy and power density are required, such as EVs [3]. Meanwhile, there exist many variants of Li-Ion battery cells with different underlying chemistries, leading to different capacities, rated power and voltage outputs, levels of safety, reliability and robustness, volume, and mass, which are used by various car manufacturers. For instance, the *Tesla Roadster* uses thousands of cells [4] with *18650* form factor. The weight of each cell is 66g. The *Mitsubishi Eclipse-EV* relies on a small number of *LEV95P* cells [5] with an unit weight of 3.5kg.

This publication is made possible by the Singapore National Research Foundation under its Campus for Research Excellence And Technological Enterprise (CREATE) programme.

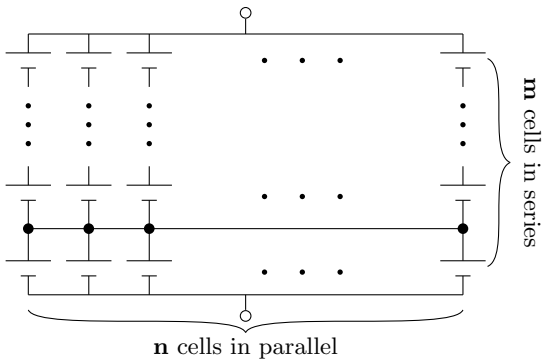

Figure 1: Functional configuration of a typical EES system with homogeneous cells in one battery pack is like a matrix.

Dimensioning and configuration of an EES system is an important design problem for EVs consisting of multiple design decisions. The following parameters need to be determined:

- the type of battery cells,
- the amount of cells **m** that are connected in series to increase the overall operating voltage, and
- the amount of cells **n** that are used in parallel for larger maximum charging and discharging current and capacity.

A typical EES system configuration with homogeneous cells placed in a battery pack is shown in Figure 1.

Four design targets of driving range, power output, installation space and system cost are identified, which make it a multi-objective optimization problem. In the meanwhile, non-quantifiable criteria like safety issues have to be taken into account separately. Moreover, in order to achieve the optimal solution, hybrid EES systems consisting of more than one type of EES element should also be considered, making the design problem even more complex [6]. For example, super-capacitors might be used to sustain primary EES elements, particularly for the purpose of regenerative braking as an example.

In a multi-objective optimization problem, a vector is considered to be a Pareto point in the objective space if all other

978-1-4799-1417-3/13/$31.00

vectors have a higher value for at least one of the objective functions, assuming all objective functions are supposed to be minimized [7]. The Pareto surface is then a set of all Pareto points, which cannot be computed efficiently in many cases. Even if it is theoretically possible to find all these points exactly, they are often of exponential size [8]. There are generally three criteria that are desirable to fulfill when solving a multi-objective optimization problem:

- the point that is found should be Pareto optimal;
- it should be possible to approach all Pareto points, even if they are, for example, located in a non-convex region;
- the set of Pareto points that are found should have an nearly even distribution over the entire objective space.

For the problem of EES system design, we need to address three additional issues. First, car manufacturers usually have specific requirements on objectives. Based on the range distribution diagram, which reflects single-trip driving distances statistically distributed among customers, a driving range constraint can be derived, which must be sustained by the EES system. From the driving profile, the power output constraint can be calculated, often with variable margins for extra acceleration capabilities depending on targeted customer groups. The installation space is constrained with a certain volume and there is also usually an upper limit for the system cost. Second, for different types of vehicles, the importance of each objective varies. For instance, the power output of a sports car is usually emphasized while the installation space for a lorry is relaxed. Third, the importance of each objective could be nonlinear to its value.

In this work, we propose an approach for optimal dimensioning and configuration of EES systems in EVs. A multi-objective optimization problem is formulated with driving range, power output, installation space and cost as design targets. A novel boundary-conditioned adaptive scalarization technique is reported. Boundaries are inserted adaptively to improve the ability of locating Pareto points. It provides a Pareto surface of evenly distributed Pareto points, presents the group of Pareto points according to different specific requirements from automotive manufacturers and also takes the fact in EES system design into account that the importance of an objective varies with different vehicles and objective function values. Hybrid EES systems are considered together with homogeneous EES systems to guarantee optimal solutions.

The organization of the paper is as follows. Section 2 describes related work regarding EES systems and multi-objective optimization. Section 3 introduces the background of EES systems and elements. The multi-objective optimization problem is formulated in Section 4. The novel adaptive scalarization technique is presented in Section 5. Section 6 reports experimental results and Section 7 contains the concluding remarks.

2. RELATED WORK

Technologies that can be applied in EVs and hybrid EVs (HEVs) have been fast progressing. Major efforts have been devoted to Li-Ion battery development, producing a wide variety of cells with superior performances in different aspects like capacity, power output, and safety. Recent progress in research of Li-Ion batteries can be found in [9, 10, 11, 12, 13]. A review of Li-Ion battery properties in the scope of EVs and HEVs is reported in [14]. At the same time, super-capacitors could be used to assist primary EES elements [15].

EES System Architecture. In [16, 17, 18, 19, 20, 21, 22, 23, 24], EES systems are discussed. Here, [18] and [22] discuss energy storage issues of HEVs while [16] reports a combination of NiMH batteries and double layer capacitors (DLC) for energy storage of an autonomous railway vehicle. Power management of a human-electric hybrid bicycle is discussed in [17]. A hybrid EES system is addressed at the circuit level in [19]. A networked charge transfer interconnect architecture for a hybrid EES system is introduced in [20]. In [21], [23], and [24], the focus is on full electric vehicles. Charge management circuits with power converters, monitoring and control circuits are proposed in [23]. An overview of charge allocation, charge replacement, and charge migration is also presented. In [24], the optimization of charge migration efficiency is discussed in more details. A balanced reconfiguration of storage banks aiming at cycle efficiency and capacity utilization enhancement is shown in [21]. Equitability reference in multi-objective optimization is applied to the design of an HEV battery and used to compute the spacing of cylindrical cells in a battery module. An optimal thermal behavior is yielded [25].

Multi-Objective Optimization. The concept of non-inferior solutions first appears in the context of economics [7] and then Pareto optimality starts to be applied to the fields of engineering and science [8]. The weighted-sum method converts a multi-objective problem into a single-objective problem and then solves it with standard techniques like Sequential Quadratic Programming [26]. In general, a uniform spread of weight parameters does not produce a uniform spread of points on the Pareto surface. What can usually be observed about this fact is that all the points are grouped in certain parts of the Pareto surface, while some portions of the trade-off curve have not been touched. Besides, non-convex parts of the Pareto set cannot be reached by minimizing convex combinations of the objective functions. ϵ-constraint is another approach to solve the multi-objective optimization problem, where one individual objective function is minimized with an upper level constraint imposed on the other objective functions, assuming that all objective functions are to be minimized [27]. The decision maker has to choose appropriate upper bounds for the constraints. Moreover, this method is not particularly efficient if the number of objective functions is greater than two.

Other methods have also been developed to solve multi-objective optimization problems. The normal boundary intersection method is presented in [28], where a series of single-objective optimizations is solved on normal lines to the utopia line. Goal programming does not pose the question of optimizing multiple objectives, but rather attempts to find specific goal values of these objectives [29]. Aiming to find one optimal point in the entire Pareto surface, multi-level programming orders all objectives according to a hierarchy. Firstly, the optima of the first objective function are found; secondly, the optima of the second most important objective are searched for; and so forth until all the objective functions have been optimized on successively smaller sets [30]. This method is particularly useful when the user is not interested in the continuous trade-off among functions. What is more, optimization problems that are solved near the end of the hierarchy can be largely constrained while less

important objective functions tend to have no influence on the overall optimal solution.

Genetic algorithms are implemented for the multi-objective problems such as gate sizing [31] and data-flow graph optimization [32]. Particle swarm optimization is reported for feature selection in cybernetics classification [33] and an automobile transmission design [34]. The major drawback is that global optima are not promised. In addition, multiple starting points might be required to better explore the Pareto surface, which could significantly increase the computational burden. A successive approach based on generation of trade-off limits has been recently presented to compute the bounded Pareto front of analog circuit sizing [35].

Adaptive Scalarization. The adaptive scalarization technique for bi-objective optimization is proposed in [36] and a new scalarization and numerical method for constructing approximated weak Pareto fronts of multi-objective optimization problems is presented in [37]. A framework of adaptive weighted aggregation based on scalarization is proposed in [38]. Coverage of solutions and computational cost strongly depend on the termination condition. In the application of resource allocation for distributed broadband heterogeneous networks, an optimal power allocation algorithm is derived based on the Lagrange optimization method and an adaptive scalarization method is used to further improve convergence speed and reduce the computational complexity [39].

While known approaches from literature consider different aspects of EES systems, the optimal dimensioning and configuration of EES systems remains an open problem. For the first time, to the best of our knowledge, we use a systematic approach to obtain an optimal solution, taking hybrid EES systems into consideration. Our method determines the type and amount of cells that should be used in an optimal EES system, together with the configuration based on various requirements. A novel boundary-conditioned adaptive scalarization technique tailored to EES system design is reported, which is able to solve both convex and concave multi-objective optimization problems. It provides a Pareto surface of evenly distributed Pareto points, presents the group of Pareto points according to different specific requirements from automotive manufacturers and also takes the fact in EES system design into account that the importance of an objective varies with different vehicles and objective function values.

3. EES SYSTEM AND ELEMENT

3.1 Performance Metrics of the EES System

Performance metrics that are commonly used to evaluate an EES element typically include specific energy, specific power, cycle life, cycle efficiency and the global emission rate [40, 41].

Specific Energy. The specific energy is calculated as the stored energy divided by the mass of the EES element and the energy density is its counterpart in term of volume. Battery cells with higher specific energy capacity or energy density are desirable for three reasons. First, larger overall energy capacity leads to a longer driving range. Second, the battery installation space is usually limited for EVs. Therefore, battery cells occupying less volume but providing similar capacities are preferred. In our optimization, the installation space is considered as both an objective and a constraint. Third, the heavier the vehicle is, the more energy is required to achieve the same driving distance, and thus it is always important to reduce the battery weight as long as the performance satisfies the requirements.

Specific Power. The specific power is calculated as the rated output power divided by the mass of the EES element and the power density is the counterpart in terms of volume. The output power requirement can be calculated with the velocity and acceleration information derived from a driving profile such as the New European Driving Cycle (NEDC) presented later in this paper. Besides propulsion, rolling friction and air resistance are also considered. Other functions utilizing battery power like air-conditioning, battery cooling, and on-board electronics need also to be taken into account. A certain margin for extra acceleration capabilities is inserted, depending on the vehicle type to design.

Cycle Life. The State-of-Health (SoH) of an EES element is a measurement of its aging. It reflects the general condition of the EES element and its ability to store and deliver energy compared to its initial state. During the lifetime of the EES element, its capacity tends to gradually deteriorate due to irreversible physical and chemical changes which take place along with the usage. The cycle life is defined as the number of cycles an EES element can perform before its capacity drops to a specific percentage (such as 75%) of its initial fully-charged capacity. It is noted that the cycle life of an EES element depends mainly on the Depth-of-Discharge (DoD) before the EES system is recharged. In general, the cycle life is increased when lowering the DoD. Li-Ion battery cells used in this work have similar cycle life, while super-capacitors usually last much longer.

Cycle Efficiency. The cycle efficiency of an EES element is the round-trip efficiency including processes of both charging and discharging. It is defined to be the product of charging efficiency and discharging efficiency, where charging efficiency is the ratio of electrical energy eventually stored in an EES element to the total energy supplied to that element during the entire charging process. Discharging efficiency is the ratio of energy output from an EES element to the total energy stored in it during the discharging process. Li-Ion battery cells and super-capacitors used in this work have similar cycle efficiency.

Global Emission Rate. EVs do not produce local CO_2 emission when driven on the road. However, CO_2 is usually emitted in the electricity generation process. This number varies with different generation methods in different countries and regions.

3.2 Characteristics Comparison of Different Energy Storage Elements

There are different types of batteries available in the market, including Lead-acid batteries, NiMH cells, and Li-Ion cells with different characteristics. Li-Ion cells are dominating the current battery market for EVs. Moreover, there exist also super-capacitors that have very high power output and cycle life. Usually, the information about cells that can be obtained from battery manufacturers contains weight, volume, capacity, rated output voltage, rated output power, maximum charging and discharging current, charging time and cost. In Table 1, four major types of Li-Ion cells and one type of supercapacitor are listed with their characteristics. They comprise Lithium-Ion cells with the *18650* form factor that are implemented in the *Tesla Roadster*, automotive-use

Table 1: Characteristics of different types of energy storage elements

Index	Battery Type	Battery Producer	Cell Mass [kg]	Cell Volume [L]	Voltage Output [V]	Capacity [Wh]	Power Output [W]	Maximum Discharging Current [A]	Cost [USD]
I	*18650* Form Factor	*SQM*	0.066	0.021	3.79	8.2	31.49	8.31	5.27
II	*HP-CT-200AH*	*Hipower Group*	6.4	4.41	3.2	640	3200	1000	236
III	Li-polymer	*Tenergy*	0.02	0.0088	3.7	3.33	33.3	9	5.51
IV	$LiFePO_4$ Cell	*All Battery*	0.394	0.212	3.2	20.8	520	162.5	36.75
V	Super-Cap	*Maxwell*	0.51	0.0023	2.7	3.04	6120	2267	51

Table 2: Comparison in performance metrics of different types of Lithium-ion cells

Comparison	Specific Energy [Wh/kg]	Energy Density [Wh/L]	Capacity per Cost [Wh/USD]
Best	Li-polymer	Super-Cap	*HP-CT-200AH*
Second	Li-Ion Cell with *18650* Form Factor	Li-Ion Cell with *18650* Form Factor	Li-Ion Cell with *18650* Form Factor
Third	*HP-CT-200AH*	Li-polymer	Li-polymer
Fourth	$LiFePO_4$	*HP-PW-200AH*	$LiFePO_4$
Worst	Super-Cap	$LiFePO_4$	Super-Cap

Comparison	Specific Power [W/kg]	Power Density [W/L]	Power per Cost [W/USD]
Best	Super-Cap	Super-Cap	Super-Cap
Second	Li-polymer	Li-polymer	$LiFePO_4$
Third	$LiFePO_4$	$LiFePO_4$	*HP-PW-200*
Fourth	*HP-CT-200AH*	Li-Ion Cell with *18650* Form Factor	Li-polymer
Worst	Li-Ion Cell with *18650* Form Factor	*HP-PW-200AH*	Li-Ion Cell with *18650* Form Factor

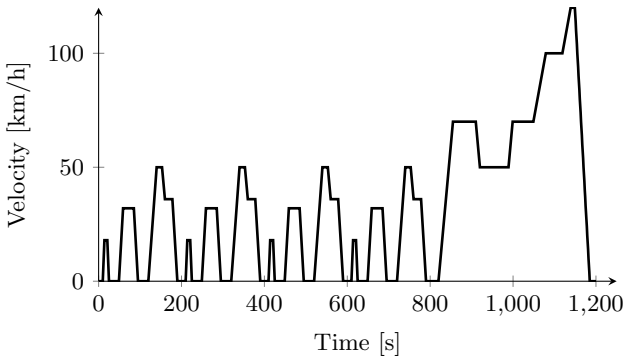

Figure 2: New European Driving Cycle consists of a series of data points representing the velocity of a vehicle versus time.

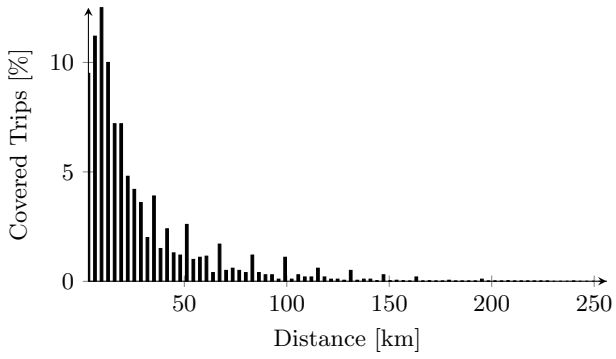

Figure 3: Driving distance distribution describes the percentage of trips that can be covered when an EES system is able to drive the vehicle to a certain driving range.

cells *HP-PW-200AH* from *Hipower Group*, Lithium-polymer cells from *Tenergy*, $LiFePO_4$ prismatic power cells from *All Battery* and super-capacitors produced by *Maxwell*. In the experiments presented in Section 6, we mainly use this list of EES elements, with three variants for each type. A comparison of these EES elements with respect to performance metrics is shown in Table 2.

4. PROBLEM FORMULATION

In EES system design, the number of cells connected in series **m** and in parallel **n** for each type of EES element are variables to be determined. **m** is usually decided based on the operating voltage that the EES system is designed to support and the output voltage of each cell. **n** is selected to fulfill requirements in power output, capacity and installation space.

Driving Cycle and Driving Distance Distribution. The EES system should be designed to fulfill customized requirements in terms of driving range, global emissions, rated power output, and installation space. The driving range and rated power output can be derived with the help of driving cycles and driving distance distribution histograms.

A driving cycle is a series of data points representing the vehicle velocity versus time, available for different countries and regions and can be used to assess EES requirements such as power output and energy consumption depending on the distance. Driving cycles can be derived either theoretically or with direct measurements of driving patterns considered as representative. The driving cycle in this work is NEDC illustrated in Figure 2, consisting of four repeated ECE-15 Urban Driving Cycles (UDC) and one Extra-Urban Driving Cycle (EUDC). The ECE-15 UDC lasts 200 seconds and the EUDC 400 seconds. As a result, the NEDC has a duration of 20 minutes in total.

To increase the market acceptance of EVs, it is important to cover as many trips as possible. For this purpose, driving distance distribution histograms [42] are used. One example of such a histogram is presented in Figure 3, illustrating the statistical relationship between the vehicle driving

range and the percentage of all possible trips that can be covered. Return trips are taken into account by considering that charging facilities are only placed at certain locations.

Vehicular and Environmental Parameters. In this work we assume the vehicle mass M_o to be constant, excluding the mass of the EES system. Additionally, we have the drag coefficient C_d, the front area A, and the air density ρ_a to calculate the air resistance as in Equation (1).

$$F_d = \frac{1}{2}\rho_a C_d A v^2(t) \tag{1}$$

With the rolling friction coefficient C_{rr}, the rolling friction force can be calculated using the mass of the EES system M_b and the gravitational constant g as in Equation (2).

$$F_f = C_{rr}(M_o + M_b)g \tag{2}$$

The air conditioning power consumption P_a, the battery cooling power consumption P_c, and the on-vehicle electronic power consumption P_g also have to be taken into account. Altogether, the overall instant power consumption can be formulated in Equation (3).

$$\begin{aligned} P(t) &= ((M_o + M_b)a(t) + \tfrac{1}{2}\rho_a C_d A v^2(t) \\ &+ C_{rr}(M_o + M_b)g)v(t) \\ &+ P_a(t) + P_c(t) + P_g(t) \end{aligned} \tag{3}$$

Here, $v(t)$ and $a(t)$ are the instant velocity and acceleration of the vehicle, respectively, that can be obtained from the driving cycle. In this context, the overall vehicle mass includes the EES system mass which itself also consumes power and energy.

Multi-Objective Optimization Model. We assume that there are p types of battery cells in total available for designers to choose from. The variables to optimize are $\{\mathbf{m_i} : i \in \{1, ..., p\}\}$ and $\{\mathbf{n_i} : i \in \{1, ..., p\}\}$, where $\mathbf{m_i} \in \mathbb{N}_0$ and $\mathbf{n_i} \in \mathbb{N}_0$ represent the number of the i-th type of battery cells in series and parallel, respectively. Given the market prices of individual cells $\{q_i : i \in \{1, ..., p\}\}$ with $q_i \in \mathbb{R}$, the objective function of the EES system cost Q is formulated in Equation (4).

$$Q = \sum_{i=1}^{p}(q_i \times \mathbf{m_i} \times \mathbf{n_i}) \tag{4}$$

The objective function on EES system installation space V_b is shown in Equation (5), where $\{s_i : i \in \{1, ..., p\}\}$ denote volume of individual cells.

$$V_b = \sum_{i=1}^{p}(s_i \times \mathbf{m_i} \times \mathbf{n_i}) \tag{5}$$

We let I_i^{max} be the maximum discharging current of the i-th type of battery cells. Then the rated power output of the EES system P_b can be calculated in Equation (6). $\{u_i : i \in \{1, ..., p\}\}$ define the rated output voltages of individual cells.

$$P_b = \sum_{i=1}^{p}(I_i^{max} \times u_i \times \mathbf{m_i} \times \mathbf{n_i}). \tag{6}$$

The vehicle driving range D that is supported by the EES system is derived in Equation (7). E_c (Equation 8) denotes the energy consumption of the driving cycle and E_b (Equation 9) is the overall capacity of the EES system while e_i is the capacity of the i-th type of battery cells. The integration on c calculates the overall driven distance of the driving cycle.

$$D = \frac{\int_c v(t)dt}{E_c} \times E_b \tag{7}$$

$$E_c = \int_c P(t)dt \tag{8}$$

$$E_b = \sum_{i=1}^{p}(e_i \times \mathbf{m_i} \times \mathbf{n_i}) \tag{9}$$

The constraints of the optimization problem are defined as follows. Intuitively, Equation (10) ensures that all variables are non-negative integers and Equation (11) sets upper and lower bounds for the operating voltage range $[U_l, U_u]$. Equation (12) states that the global emission of CO_2 by the EES system cannot exceed a certain threshold G_o, where g_i denotes the CO_2 emission of the i-th type of cells.

$\forall i \in \{1, ..., p\}$:

$$\mathbf{m_i} \in \mathbb{N}, \mathbf{n_i} \in \mathbb{N} \tag{10}$$

$\forall i \in \{1, ..., p\}$:

$$U_l \leq u_i \times \mathbf{m_i} \leq U_u \tag{11}$$

$$\sum_{i=1}^{p}(g_i \times \mathbf{m_i} \times \mathbf{n_i}) \leq G_o \tag{12}$$

Specific and Adaptive Requirements in EES System Design. In EES system design, on top of the optimization model formulated above, there are usually some additional specific and adaptive requirements from car manufacturers, depending on targeted groups of customers and vehicle types. Values of the objective functions become meaningless when crossing certain boundaries. Constraints on the four objectives are shown in Equation (13) to Equation (16), which restrict the feasible region of the parameter space.

Denoting Q^o and V_b^o to be the boundaries of system cost and installation space respectively, it is intuitive that the cost cannot be too high and that the space cannot be too large. Regarding the power output, it has to be ensured that at every instant, the power provided by the EES system P_b is larger than the power requirement $P(t)$. We remark that a certain margin P_m is inserted for extra acceleration capabilities. As for the driving range, the target D_o is derived from the driving distance distribution diagram so that a certain percentage of all possible trips can be covered by the EES system.

$$Q \leq Q^o \tag{13}$$

$$V_b \leq V_b^o \tag{14}$$

$$P_b \geq \max_t\{P(t)\} + P_m \tag{15}$$

$$D \geq D_o \tag{16}$$

In the EES system design, the importance of different objectives varies. In the following, importance factors of objectives and the optimal solution under a specific set of importance factors are described.

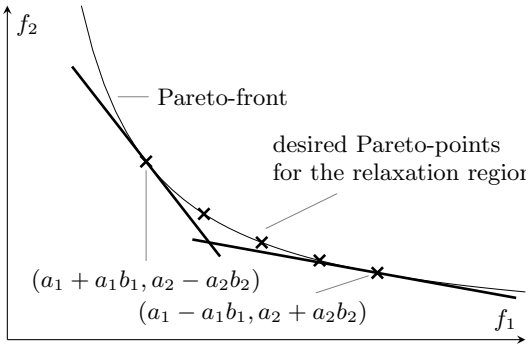

Figure 4: Desired Pareto points within the relaxation region of importance factors based on specific requirements are illustrated in bi-objective optimization. Two end points correspond to two sets of importance factors $(a_1 - a_1b_1, a_2 + a_2b_2)$ and $(a_1 + a_1b_1, a_2 - a_2b_2)$, respectively.

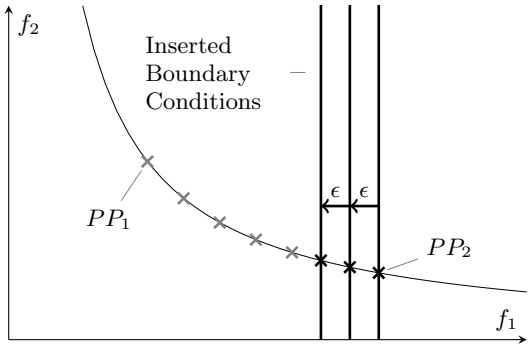

Figure 5: When the distribution density of Pareto points corresponding to the relaxation region is worse than average, additional boundary conditions are inserted in an adaptive step of ϵ to find Pareto points that are difficult to locate with a normal scalarization technique.

We first consider bi-objective optimization, where there are two normalized objectives f_1 and f_2 to be minimized with two importance factors a_1 and a_2. The relative importance factor is defined as $a_{12} = \frac{a_1}{a_2}$. Denoting $\Delta d_1 = f_1(d') - f_1(d)$ and $\Delta d_2 = f_2(d') - f_2(d)$, it is stated that d is the optimal solution in the design space $\mathbb{D}$ under the set of importance factors $\{a_1, a_2\}$ if its corresponding point in the objective space $\mathbb{O}$ is on the Pareto surface $\mathbb{P}$ and there is no such point d' in $\mathbb{D}$, that satisfies Equation (17) and whose corresponding point in $\mathbb{O}$ is on $\mathbb{P}$.

$$a_{12}\Delta d_1 < -\Delta d_2 \tag{17}$$

If f_1 is twice as important as f_2, then a new point is considered better if the improvement in f_1 is at least half of the degradation in f_2 or the improvement in f_2 is at least twice the degradation in f_1.

Then we can extend it to the optimization problem where there are w normalized objective functions $\{f_j : j \in \{1, ..., w\}\}$ to be minimized. Each objective function f_j is assigned an importance factor a_j and we have

$$\sum_{j=1}^{w} a_j = 1 \tag{18}$$

Similarly, it is stated that d is the optimal solution if its corresponding point in $\mathbb{O}$ is on $\mathbb{P}$ and there is no such point d', which satisfies Equation (19) and whose corresponding point in $\mathbb{O}$ is on $\mathbb{P}$.

$$\sum_{j=1}^{w} a_j \Delta d_j < 0 \tag{19}$$

As discussed earlier, the importance factor of the same objective can vary when it takes different values. In Section 5, it will be presented how such a problem can be solved with our proposed adaptive scalarization technique.

5. OPTIMIZATION SOLUTION WITH ADAPTIVE SCALARIZATION TECHNIQUE

Without loss of generality, we assume that there are w objectives to minimize on p variables in the design space $\mathbb{D}$. There are r constraints on variables and w boundaries on objectives. Each objective has an importance factor. The general problem that our proposed adaptive scalarization technique is able to solve is formulated in Equation (20).

$$\begin{gathered} \min_{\mathbb{D}} \{f_j : j \in \{1, ..., w\}\} \\ \text{subject to} \\ \{c_i : i \in \{1, ..., r\}\} \\ \{o_j : j \in \{1, ..., w\}\} \\ \{a_j : j \in \{1, ...w\}\} \\ \sum_{j=1}^{w} a_j = 1 \end{gathered} \tag{20}$$

First, we normalize all objectives to the same scale so that the values are comparable. Different normalization methods can be applied and in the scope of EES system design, the difference between the maximum and minimum of each objective is used as the normalization factor as shown in Equation (21).
$\forall j \in \{1, ..., w\}$:

$$f'_j = \frac{f_j}{\max f_j - \min f_j} \tag{21}$$

Denoting $\{b_j : j \in \{1, ..., w\}\}$ to be a set of relaxation factors, which determine to what extend the importance factors can be relaxed, for any objective f_j, we can construct a relaxation region $[-a_jb_j, a_jb_j]$. Only Pareto points under this region of importance factors are of interest. For any importance factor in this region a'_j, the corresponding importance factors of other objectives a'_k are calculated in Equation (22). This concept is illustrated in Figure 4 in bi-objective optimization.

$$a'_k = a_k \frac{1 - a'_j}{1 - a_j} \tag{22}$$

Then we can construct a function as shown in Equation (23).

$$f = \sum_{j=1}^{w} a'_j f'_j \tag{23}$$

We can solve Equation (23) with Equation (22) and constraints in Equation (20). There exist many methods for it. One of them is Sequential Quadratic Programming, which is able to handle significant non-linearities. For each objective, two points on $\mathbb{P}$ corresponding to two end points of the relaxation region are obtained and we denote the Euclidean distance between them with d_j. The Euclidean distance d_j^o between the two points derived with the maximum and minimum importance of f_j, respectively is calculated in Equation (24). We remark that the full set of importance factors is updated according to Equation (22).

$$d_j^o = || \min_{a'_j=1} f, \min_{a'_j=0} f|| \tag{24}$$

Algorithm 1: This algorithm finds a list of Pareto points that satisfy all requirements and have a representative distribution.

Input: The optimization problem in Equation 20
Output: A list of Pareto points $\mathbb{PP}$

1 Normalization: Equation 21
2 Function Construction: Equation 23
3 **for** $j \leftarrow 1$ ***to*** w **do**
4 $a'_j = a_j + a_j b_j$
5 **for** $k \leftarrow 1$ ***to*** w *excluding* j **do**
6 Calculate a'_k as in Equation 22
7 Solve Equation 23 for Pareto Point I PP_1
8 Update $\mathbb{PP}$
9 $a'_j = a_j - a_j b_j$
10 Update a'_k as in Line 5 to 6
11 Solve Equation 23 for Pareto Point II PP_2
12 Update $\mathbb{PP}$
13 $d_j = ||PP_1, PP_2||$
14 Calculate d_j^o as in Equation 24
15 **while** $2a_j b_j < \frac{d_j}{d_j^o}$ **do**
16 Introduce $f'_j < f'_j(PP_2) - \epsilon$ to Equation 23
17 Repeat Line 9 to 12 and PP_2 gets updated
18 Increase ϵ
19 Assign a value in $[a_j - a_j b_j, a_j + a_j b_j]$ to a'_j
20 Update a'_k as in Line 5 to 6
21 Solve Equation 23 for a new Pareto point
22 Update $\mathbb{PP}$
23 Repeat Line 19 to 22 when necessary
24 **return** *A list of Pareto points* $\mathbb{PP}$

If $2a_j b_j > \frac{d_j}{d_j^o}$, it means that the distribution density of Pareto points corresponding to this relaxation region is better than average. In other words, more values of a'_j can be adaptively taken within this relaxation region with importance factors of other objectives a'_k updated accordingly so that Equation (23) can be solved iteratively for points in $\mathbb{D}$ as Pareto solutions that fulfill all requirements.

If $2a_j b_j < \frac{d_j}{d_j^o}$, it means that the distribution density is small and that certain representative Pareto points could be missing. In order to discover them, we introduce a new

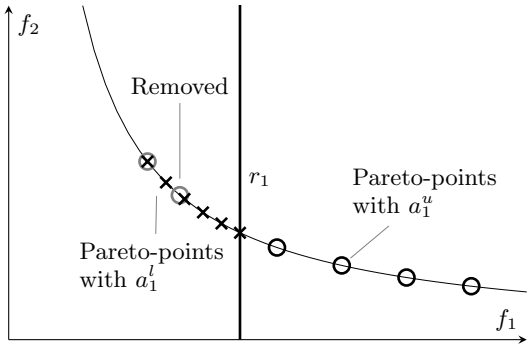

Figure 6: For the importance factor a_1^l corresponding to the lower region, a boundary condition is inserted at r_1; for a_1^u in the upper region, solution points below r_1 are removed.

boundary condition $f'_j < f'_j(d_j^-) - \epsilon$, where d_j^- is the solution point in $\mathbb{D}$ corresponding to the least importance of f_j within the relaxation region and $\epsilon > 0$ as shown in Figure 5. ϵ can be adaptively updated based on requirements. After this boundary condition is established, we can solve Equation (23) iteratively until enough representative Pareto points are located. The whole process is then iterated over all objectives, which is shown in Algorithm 1.

Algorithm 2: This algorithm shows how to locate desired Pareto points when at least one objective function has two importance factors.

Input: $\{f'_j : j \in \{1, ..., w\}\}, \{a_j^u : j \in \{1, ..., w\}\}, \{a_j^l : j \in \{1, ..., w\}\}, \{r_j : j \in \{1, ..., w\}\}$
Output: A set of Pareto points

1 **for** *All combinations of importance factors* **do**
2 **for** $j \leftarrow 1$ ***to*** w **do**
3 **if** $a_j = a_j^l$ **then**
4 Insert $f'_j < r_j$ to the optimization problem
5 Solve the optimization problem as in Algorithm 1
6 **for** $j \leftarrow 1$ ***to*** w **do**
7 **if** $a_j = a_j^u$ **then**
8 **for** *All solution points* **do**
9 **if** $f'_j < r_j$ **then**
10 Remove the point from the solution set
11 **return** *A set of Pareto points*

In EES system design, sometimes the importance of an objective differs when it takes different values and thus one objective function needs to have two importance factors. For the importance factor corresponding to the lower region with smaller values of an objective function a_j^l, we can insert an additional boundary condition, which still finds Pareto points. For the importance factor corresponding to the upper region with larger values of an objective function a_j^u, we apply it for both regions and then remove the solution points that lie in the lower region. This process is repeated for all possible combinations of importance factors as shown in Algorithm 2 and illustrated in Figure 6, where

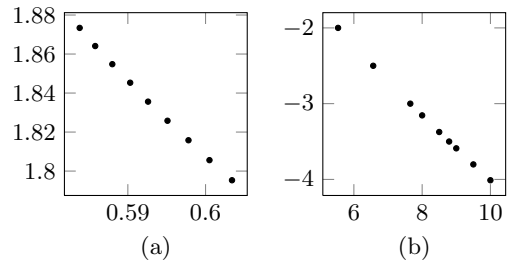

Figure 7: The two graphs illustrate Pareto points in the objective space corresponding to two different sets of importance factors in the first numerical example.

$\{r_j : j \in \{1, ...w\}\}$ is the set of threshold values between these two regions.

For the sake of completeness, we discuss briefly how to deal with a situation when one objective has more than two importance factors, it is rather unrealistic in EES system design though. We assume that one objective has three importance factors a_j^l, a_j^m, and a_j^u and two threshold values r_j^l and r_j^u. First, to obtain solutions corresponding to a_j^l, the boundary condition of $f_j' < r_j^l$ is inserted. Second, the boundary condition of $f_j' < r_j^u$ is inserted and solutions located in the lower region are removed. The remaining solutions are then for a_j^m. Third, for solutions with a_j^u, no boundary condition is inserted and solution points lying in the middle and lower regions are erased.

6. EXPERIMENTAL RESULTS

In this section, we are going to demonstrate that our proposed adaptive scalarization technique is effective with numerical and practical experiments. In the first numerical example, the optimization problem is shown in Equation (25) with five variables and two objectives.

$$\begin{gathered}
\min f_1, f_2 \\
f_1 = x_1^2 + x_2^2 + x_3^2 + x_4^2 + x_5^2 \\
f_2 = 3x_1 + 2x_2 - \tfrac{x_3}{3} + 0.01(x_4 - x_5)^3 \\
\text{subject to} \\
\{x_i \in \mathbb{R} : i \in [1, 5]\} \\
x_1 + 2x_2 - x_3 - 0.5x_4 + x_5 = 2 \\
4x_1 - 2x_2 + 0.8x_3 + 0.6x_4 + 0.5x_5^2 = 0 \\
x_1^2 + x_2^2 + x_3^2 + x_4^2 + x_5^2 \leq 10
\end{gathered} \tag{25}$$

Since this is a numerical example, no normalization is required. In the first case, we assume a set of importance factors $\{0.8, 0.2\}$ and the relaxation factor on f_2 to be 0.1. After calculating the Euclidean distance, it is noticed that the distribution density of Pareto points is better than average and thus we proceed to generate other solutions within this relaxation region. The result is shown in Figure 7 (a). In the second case, we move to another region with importance factors $\{0.2, 0.8\}$. The entire region only produces one Pareto point $(10, -4.0111)$ and thus we know that this region needs further exploration without calculation. After implementing Algorithm 1, the result is presented in Figure 7 (b). This example demonstrates the ability of our proposed method to locate a set of Pareto points based on different sets of importance factors. We remark that an even distribution is achievable with a more carefully chosen set of ϵ if necessary.

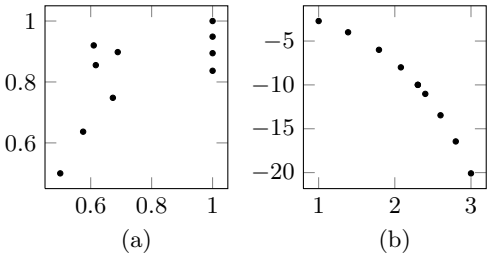

Figure 8: Experimental results of the second numerical example. The parameter space is shown in (a) and the objective space is shown in (b).

Table 3: Experimental results of the two cases in the EES system design are shown. S is for series and P is for parallel.

Case	I	II
Vehicle Type	Pickup Truck	Sports Car
Importance	Cost+Distance	Power+Volume
Type I (S)	0	106
Type I (P)	0	58
Type II (S)	125	0
Type II (P)	1	0
Type III (S)	0	0
Type III (P)	0	0
Type IV (S)	0	0
Type IV (P)	0	0
Type V (S)	0	0
Type V (P)	0	0
Cost [kUSD]	29.5	32.4
Volume [L]	551.3	129.5
Power [kW]	400	193.6
Distance [km]	268.9	179.9

In the second numerical example, we look at a non-convex problem as shown in Equation (26).

$$\begin{gathered}
\min f_1, f_2 \\
f_1 = x_1 + 2x_2^2 \\
f_2 = e^{x_1 + 2x_2^2} \\
\text{subject to} \\
0.5 \leq x_i \leq 1, i = 1, 2
\end{gathered} \tag{26}$$

The results are shown in Figure 8 with the parameter space presented on the left and objective space on the right. It is seen that our proposed method is able to handle non-convex optimization problems.

Now we apply our approach in EES system design. The five types of EES elements shown in Table 1 are used with three variants for each type. In the first case, we consider a pickup truck, for which the cost is sensitive, the driving range is important, there is relatively large installation space

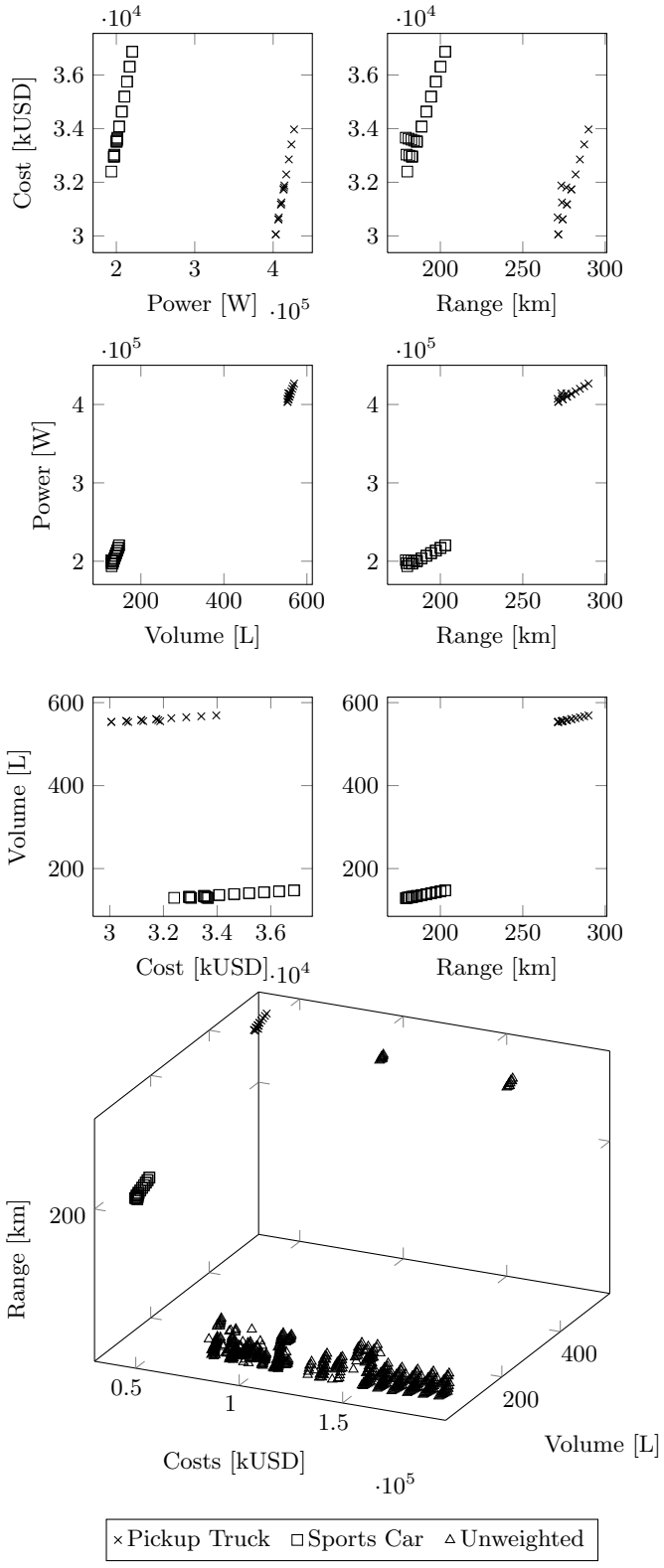

Figure 9: Results of the presented case study are presented. Six projections of the objective space as well as a three dimensional plot omitting the power output with unweighted Pareto points are illustrated.

and no extra power output is necessary. The result in Table 3 shows that the optimal type of EES element for a pickup truck is *HP-CT-200AH*. 125 of such cells are placed in series in the EES system with the cost of 29.5k USD and a driving range of more than 250 km. The volume required is about half a cube meter and 400 kW of power output is good enough.

In the second case, we consider a sports car with nonlinear importance factors. In the starting stage of EES system design, usually a certain amount of space is allocated for battery installation and it is advised to keep it within this space. We assume that this number is 200 L in this situation and thus the importance factor of installation space is high when its value is above 200 L. In other words, the optimization process is better motivated to go for a solution with less installation space when it is above this threshold. By the same token, the importance of power output drops when it is already above 100 kW. From the result, we can see that the battery cell with *18650* form factor from *SQM* is chosen. 6148 such cells are placed in a matrix, with the cost of 32.4k USD and a driving range of 180 km. The installation space is 130 L and the power output is 190 kW. This ensures enough extra acceleration capabilities for a wide range of driving speeds.

The Pareto points of both cases are illustrated in Figure 9. Six projections are presented to show relationships between any two objectives. A more generalized three-dimensional graph of Pareto points is plotted with power output omitted. This graph includes those Pareto points without specific sets of importance factors. It is remarked that the runtime for these test cases is in the scale of minutes. Scalability is not a sensitive issue since EES system design is an offline task within the vehicle design cycle that could last for years.

7. CONCLUSION

In this work, we propose an approach for optimal dimensioning and configuration of EES systems in EVs. A multi-objective optimization problem is formulated with driving range, power output, installation space and cost as design targets. We report a novel boundary-conditioned adaptive scalarization technique to solve both convex and concave problems. It provides a Pareto surface of evenly distributed Pareto points, presents the group of Pareto points according to different specific requirements from automotive manufacturers and also takes the fact in EES system design into account that the importance of an objective varies with its values. Numerical and practical experiments prove that our proposed approach produces optimal solutions of what types of EES elements should be implemented in the EES system and the configuration, given the targeted vehicle type, desired performances and cost, available EES elements and the characteristics, vehicular dynamics, and environmental parameters.

8. REFERENCES

[1] M. Lukasiewycz et al. System Architecture and Software Design for Electric Vehicles. In *Proc. of DAC*, 2013.

[2] S. Lukic, J. Cao, R. Bansal, F. Rodriguez, and A. Emadi. Energy Storage Systems for Automotive Applications. *IEEE Transactions on Industrial Electronics*, 55(6):2258–2267, June 2008.

[3] J. Molenda. Li-ion Batteries for Electric Vehicles. *Annales UMCS, Chemistry*, 66:23–36, 2011.

[4] G. Berdichevsky, K. Kelty, JB Straubel, and E. Toomre. The Tesla Roadster Battery System. *Tesla Motors Inc*, 2006.

[5] N. Takeda, S. Imai, Y. Horii, and H. Yoshida. Development of High-performance Lithium-ion Batteries for Hybrid Electric Vehicles. *Mitsubishi Motors Technical Review*, pages 68–72, 2003.

[6] F. Koushanfar. Hierarchical hybrid power supply networks. In *Proc. of DAC*, 2010.

[7] V. Pareto. *Manuale di Economia Politica*. Societa Editrice Libraria, Milano, Italy, 1906.

[8] W. Stadler. A Survey of Multicriteria Optimization or the Vector Maximum Problem. *Journal of Optimization Theory and Applications*, 29(1):1–52, September 1979.

[9] W. Cui and D. Tang. Electrospun Poly (Lithium 2-acrylamido-2-methylpropanesulfonic acid) Fiber-Based Polymer Electrolytes for Lithium-ion Batteries. *Journal of Applied Polymer Science*, 126:510–518, 2012.

[10] B. Lalia, Y. Samad, and R. Hashaikeh. Nanocrystalline-Cellulose-Reinforced Poly (vinylidenefluoride-co-hexafluoropropylene) Nanocomposite Films as a Separator for Lithium Ion Batteries. *Journal of Applied Polymer Science*, 126:441–447, 2012.

[11] B. Lee, S. Nam, and J. Choi. Anodic TiO_2 Nanotubes as Anode Electrode in Li-air and Li-ion Batteries. *Current Applied Physics*, 12:1580–1585, 2012.

[12] Y. Qiao, X. Wang, Y. Mai, X. Xia, J. Zhang, C. Gu, and J. Tu. Freeze-drying Synthesis of $Li_3V_2(PO_4)_3/C$ Cathode Material for Lithium-ion Batteries. *Journal of Alloys and Compounds*, 536:132–137, 2012.

[13] S. Yoon, K. Jung, C. Jin, and K. Shin. Synthesis of Nitrided MoO_2 and Its Application as Anode Materials for Lithium-ion Batteries. *Journal of Alloys and Compounds*, 536:179–183, 2012.

[14] T. Duong. A Review of Lithium-ion Battery Properties of Plug-in Hybrid and Electric Vehicles in Light of Seminal Assumptions on the Viability of V2G. In *Proc. of ISGT*, 2012.

[15] B. Dakyo and H. Gualous. Polynomial Control Method of DC/DC Converters for DC-Bus Voltage and Currents Management-Battery and Supercapacitors. *IEEE Transactions on Power Electronics*, 27(3):1455–1467, 2012.

[16] J. Bocker, K. Witting, A. Seifried, and O. Znamenshchykov. Optimal Energy Management for a Hybrid Energy Storage System Combining Batteries and Double Layer Capacitors. In *Proc. of ECCE*, pages 1640–1647, 2009.

[17] R. Hsu, C. Liu, and D. Chan. A Reinforcement-Learning-Based Assisted Power Management with QoR Provisioning for Human-Electric Hybrid Bicycle. *IEEE Transactions on Industrial Electronics*, 59(8):3350–3359, 2012.

[18] E. Karden, S. Ploumen, B. Fricke, T. Miller, and K. Snyder. Energy Storage Devices for Future Hybrid Electric Vehicles. *Journal of Power Sources*, 168(1):2–11, 2007.

[19] A. Khaligh and Z. Li. Battery, Ultracapacitor, Fuel Cell, and Hybrid Energy Storage Systems for Electric, Hybrid Electric, Fuel Cell, and Plug-In Hybrid Electric Vehicles: State of the Art. *IEEE Transactions on Vehicular Technology*, 59(6):2806–2814, 2010.

[20] Y. Kim, S. Park, N. Chang, Q. Xie, Y. Wang, and M. Pedram. Networked Architecture for Hybrid Electrical Energy Storage Systems. In *Proc. of DAC*, 2012.

[21] Y. Kim, S. Park, Y. Wang, and Q. Xie. Balanced Reconfiguration of Storage Banks in a Hybrid Electrical Energy Storage System. In *Proc. of ICCAD*, pages 624–631, 2011.

[22] T. Markel and A. Simpson. Plug-In Hybrid Electric Vehicle Energy Storage System Design. In *Proc. of Advanced Automotive Battery Conference*, 2006.

[23] M. Pedram, N. Chang, Y. Kim, and Y. Wang. Hybrid Electrical Energy Storage Systems. In *Proc. of ISLPED*, pages 363–368, 2010.

[24] Y. Wang, Y. Kim, Q. Xie, N. Chang, and M. Pedram. Charge Migration Efficiency Optimization in Hybrid Electrical Energy Storage (HEES) Systems. In *Proc. of ISLPED*, pages 103–108, 2011.

[25] B. Dandurand, P. Guarneri, G. Fadel, and M. Wiecek. Equitable Multi-Objective Optimization Applied to the Design of a Hybrid Electric Vehicle Battery. *Journal of Mechanical Design*, 135(4), 2013.

[26] I. Das and J. Dennis. A Closer Look at Drawbacks of Minimizing Weighted Sums of Objectives for Pareto Set Generation in Multicriteria Optimization Problems. *Structural Optimization*, 14(1):63–69, August 1997.

[27] R. Steuer. *Multiple Criteria Optimization: Theory, Computation and Application*. Wiley, New York, 1986.

[28] I. Das and J. Dennis. Normal-Boundary Intersection: A New Method for Generating the Pareto Surface in Nonlinear Multicriteria Optimization Problems. *SIAM Journal on Optimization*, 8(3):631–657, 1998.

[29] A. Charnes, W. Cooper, and R. Ferguson. Optimal Estimation of Executive Compensation by Linear Programming. *Management Science*, 1(2):138–151, 1955.

[30] G. Saharidis and M. Ierapetritou. Resolution Method for Mixed Integer Bi-Level Linear Problems Based on Decomposition Technique. *Journal of Global Optimization*, 44(1):29–51, 2009.

[31] L. Xiao and W. Sheng and Z. Mao. Soft Error Optimization of Standard Cell Circuits Based on Gate Sizing and Multi-Objective Genetic Algorithm. In *Proc. of DAC*, pages 502–507, 2009.

[32] B. Landwehr. A Genetic Algorithm Based Approach for Multi-Objective Data-Flow Graph Optimization. In *Proc. of ASPDAC*, pages 355–358, 1999.

[33] B. Xue, M. Zhang, and W. Browne. Particle Swarm Optimization for Feqture Selection in Classification: A Multi-Objective Approach. *IEEE Transactions on Cybernetics*, pages 1–16, 2013.

[34] Y. Wu and Q. Fan and F. Wang. Application of Multi-Objective Particle Swarm Optimization in Automobile Transmission Design. In *Proc. of ICIC*, pages 215–218, 2010.

[35] D. Mueller-Gritschneder, H. Graeb, and U. Schlichtmann. A Successive Approach to Compute the Bounded Pareto Front of Partical Multi-objective Optimization Problems. *SIAM Journal on Optimization*, 20(2):915–934, 2009.

[36] I. Kim and O. Weck. Adaptive Weighted-Sum Method for Bi-Objective Optimization: Pareto Front Generation. *Structural and Multidisciplinary Optimization*, 29(2):149–158, 2005.

[37] J. Dutta and C. Kaya. A New Scalarization and Numerical Method for Constructing the Weak Pareto Front of Multi-Objective Optimization Problems. *Optimization*, 60(8-9):1091–1104, 2011.

[38] N. Hamada and Y. Nagata and S. Kobayashi and I. Ono. On Scalability of Adaptive Weighted Aggregation for Multiobjective Function Optimization. In *Proc. of IEEE Globecom Workshops*, pages 1102–1106, 2012.

[39] N. Li and C. Xing and Z. Fei and J. Kuang. Adaptive Multi-Objective Optimization for Distributed Heterogeneous Networks. In *Proc. of IEEE Globecom Workshops*, pages 1102–1106, 2012.

[40] D. Linden and T. Reddy. *Handbook of Batteries, Third Edition*. McGraw-Hill, 2002.

[41] M. Uno and K. Tanaka. Accelerated Charge-Discharge Cycling Test and Cycle Life Prediction Model for Supercapacitors in Alternative Battery Applications. *IEEE Transactions on Industrial Electronics*, 59(12):4704–4712, 2012.

[42] R. Haaren. Assessment of Electric Cars' Range Requirements and Usage Patterns based on Driving Behavior Recorded in the National Household Travel Survey of 2009. *Technical Report*, 2009.